THE UNIVERSITY of EDINBURGH

Edinburgh Research Explorer

Hinge location and apical drill holes in opening wedge high tibial osteotomy: a Finite Element Analysis

OPEN ACCESS

Title Page

Hinge location and apical drill holes in opening wedge high tibial osteotomy: a Finite Element Analysis

Miss Anna Boström [1]

Mr Anish K Amin [2]

Mr Gavin J Macpherson [2]

Prof Pankaj Pankaj [3]

Ms Chloe EH Scott [2, 3]

1. School of Engineering, The University of Edinburgh, UK

2. Department of Orthopaedics, Royal Infirmary of Edinburgh, UK

3. School of Engineering, Institute for Bioengineering, The University of Edinburgh, UK

Corresponding Author:

Chloe EH Scott

Department of Orthopaedics, Royal Infirmary of Edinburgh, 51 Little France Crescent, Edinburgh EH16 4SA, UK.

Tel: +44 (0)7989 550 456

Email: chloeehscott@yahoo.co.uk

Author Contributions Statement:

Miss Anna Boström: Model creation and analysis, Data interpretation, Manuscript preparation.

Mr Anish K Amin: Concept, Data interpretation, Manuscript preparation.

Mr Gavin J Macpherson: Concept, Data interpretation, Manuscript preparation.

Prof Pankaj Pankaj: Concept, Model development, Data interpretation, Manuscript preparation

Ms Chloe EH Scott: Concept, Model development, Data interpretation, Manuscript preparation

Hinge location and apical drill holes in opening wedge high tibial osteotomy: a Finite Element Analysis

Abstract

At the time of medial opening wedge high tibial osteotomy (HTO) to realign the lower limb and offload medial compartment knee osteoarthritis, unwanted fractures can propagate from the osteotomy apex. The aim of this study was to use finite element (FE) analysis to determine the effect of hinge location and apical drill holes on cortical stresses and strains in HTO.

A monoplanar medial opening wedge HTO was created above the tibial tuberosity in a composite tibia. Using the FE method, intact lateral hinges of different widths were considered (5, 7.5 and 10mm). Additional apical drill holes (2, 4 and 6mm diameters) were then incorporated into the 10mm hinge model. The primary outcome measure was maximum principal strain in the cortical bone surrounding the hinge axis. Secondary outcomes included the force required for osteotomy opening, minimum principal strain and mean cortical bone stresses (maximum principal/minimum principal/von Mises).

Larger intact hinges (10mm) were associated with higher cortical bone maximum principal strain and stress, lower minimum principal strain/stress and required greater force to open. Lateral cortex strain concentrations were present in all scenarios, but extended to the joint surface with the 10mm hinge. Apical drill holes reduced the mean cortical bone maximum principal strain adjacent to the hinge axis: 2mm hole 6% reduction; 4mm 35% reduction; 6mm 55% reduction. Incorporating a 4mm apical drill hole centred 10mm from the intact lateral cortex maintains a cortical bone hinge, minimises cortical bone strains and reduces the force required to open the HTO thus improving control.

Introduction

Osteoarthritis (OA) is the most common form of arthritis in the UK[1], and in much of the developed world[2,3]. The knee joint is most susceptible to developing OA[4] and this may be predisposed by obesity, trauma, malalignment and age. Physiologically, the medial compartment of the knee receives a greater proportion of body weight than does the lateral[5]. This imbalance is amplified in varus malalignment accelerating medial cartilage wear. In such patients with isolated medial compartment OA, realignment with high tibial osteotomy (HTO) is an alternative surgical treatment to unicompartmental (UKA) or total knee arthroplasty (TKA). Altering the mechanical axis of the lower limb so that it passes through the unaffected lateral compartment of the knee relatively offloads the diseased medial compartment reducing pain. HTO is indicated in end-stage unicompartmental knee OA in active patients <60years old who in general display greater dissatisfaction following TKA and higher revision rates[6].

Lower limb realignment using HTO can be performed using either opening or closing wedge techniques, with either monoplanar or biplanar osteotomies depending on the anatomical relationship to the tibial tuberosity. Medial opening wedge HTO can be complicated by intraoperative lateral hinge fractures at a rate of 14-25% (Takeuchi 7, 8, 9, Kumugai 10). These fractures most commonly propagate laterally and are defined as Takeuchi Type I (73% of fractures) but can alternatively propagate inferiorly as Type II (19%) or vertically to the lateral tibial plateau joint surface as Type III fractures (8%) (Takeuchi 7). Such fractures affect immediate construct stability, tibial slope, alignment offset and the correction obtained and are known to increase time to union, risk of non-union and stresses and strains within the fixation plate thus increasing the potential for fatigue failure of fixation requiring additional surgery [7-11]. Vertical crack propagation (Type III fractures) is particularly serious as it creates intra-

articular incongruity of the lateral plateau onto which the mechanical axis is being shifted. The

risk of lateral fracture at medial opening wedge HTO has been shown to be reduced by inserting

K-wires which cross at the desired hinge location in an experimental cadaveric study [12]. Others

have suggested using an apical drill hole for the same purpose[13]. Apical drill holes have been

incorporated into the design of proprietary HTO jigs, which can be patient specific, to minimise

the risk of iatrogenic fracture in addition to aiding osteotomy accuracy and precision.

The aim of this finite element (FE) study was to determine the effect of surgical technique on

the risk of fracture propagation in monoplanar opening wedge HTO. Specifically the effect of

hinge axis location (depth and width) and drill hole augmentation on proximal tibial cortical

bone stresses and strains was investigated.

Methods

An FE model previously experimentally validated using Digital Image Correlation (±4.5%

error) and Acoustic Emissions (±12.5% error)[14,15] was used. This consisted of a third

generation left composite tibia with cortical and cancellous parts. Analysis was performed

using ABAQUS CAE Version 6.12 (Simulia, Dassault Systemes, Walthan, USA). Anatomical

axes were defined in coronal and sagittal planes [14] The tibia was sectioned distally 200mm

below the intercondylar eminence to reduce computational effort.

Material Properties

Both cancellous (Elastic modulus 0.155GPa, Poisson's ratio 0.3) and cortical bone (Elastic

modulus 16.7GPa, Poisson's ratio 0.3) were assumed to have homogeneous, isotropic and

elastic material properties for the purpose of analysis [14-18]. Tie constraints were used to bond cancellous and cortical bone.

Osteotomy Geometry

A monoplanar medial opening wedge osteotomy was created by removing 2mm of bone along the length of the osteotomy (Figure 1) as would occur when using a saw. This was placed above the tibial tuberosity at an angle of 15° to the plane perpendicular to the coronal plane anatomical axis, and parallel to the posterior tibial slope in the sagittal plane in the direction of the fibular head (Figure 1). The initial model retained an intact hinge of lateral bone of width 10mm (10.19mm) in the transverse plane (figure 2). To investigate different widths of intact hinge, the osteotomy was extended along the same plane to evaluate intact hinge widths of 7.5mm (7.69mm) and 5mm (5.19mm). The vertical distance from the osteotomy apex to the tibial plateau was 15-20mm. To investigate the effect of a drill hole at the hinge axis, the model with the 10mm intact lateral hinge was altered (Figure 3). The centre point of the lateral edge of the osteotomy apex was defined as the hinge axis and the centre of drill holes of 2mm, 4mm, and 6mm diameters were placed concentric with this axis. These drill holes resulted in intact lateral hinge widths of 9.19 mm (2mm drill), 8.19mm (4mm drill) and 7.19mm (6mm drill).

Mesh

The proximal tibia of each model was partitioned into four parts according to the osteotomy geometry: 2mm medial from the hinge axis and 2mm proximal to upper surface of the osteotomy cut (Figure 4). This defined 4 regions of interest (ROIs) with ROI 1 at the tip of the osteotomy containing all elements adjacent to the hinge axis and ROI 2 running vertically

above it **(Figure 4)**. A mesh comprising linear tetrahedral elements was generated. The generated mesh was biased according to the partitioning with smaller elements in ROI 1 and 2 where elevated stresses/strains were expected (Figure 4): ROI 1 internodal distance 1mm; ROI 2 1mm; ROI3 2mm ; and ROI4 4mm. Average element size was 2.5 mm. The addition of drill holes required finer mesh with internodal distance of 0.6mm in ROIs 1 and 2 (Figure 3). The number of elements in each model is given in Table 1.

Boundary Conditions and Loading

Loading was applied as prescribed displacements to open the osteotomy. The upper cut surface of the osteotomy was fully restrained and a vertical displacement of 10mm was applied to nodes at the medial periphery of the cortical bone on the lower cut surface, decreasing linearly along the osteotomy to 0mm at the hinge axis. Other than these prescribed restraints and displacements at the osteotomy surfaces, no other boundary conditions were applied. With the lack of positional restraints on all but the upper osteotomy surface this created an arc of displacement about the hinge axis. As significant displacements were applied, the analyses conducted were geometrically non-linear.

Outcome measures

ROI 1 contained the hinge axis and was thus expected to contain the elements experiencing the largest stresses and strains when the osteotomy was distracted. ROI 1 also included the areas in which Type I (lateral) and II (inferior) fractures occur. According to the crack tip stress theory[13] for an infinitesimally fine crack tip (zero radius) wedge opening would cause stress at

the apex of the crack tip to approach infinity. The geometry considered did not have a fine crack. Crack tip proximity however can give falsely elevated peak stresses and strains, therefore the mean stress/strain over ROI 1 was selected as an outcome measure in preference. Cortical bone stresses and strains were computed.

The primary outcome measure was the mean cortical bone maximum principal strain (positive values indicate tension) in ROI 1. Secondary outcomes included the force required to distract the osteotomy, mean minimum principal strain (negative values indicate compression) in ROI 1 and von Mises stress measured around the osteotomy apex – the hinge axis.

Results

Width of intact hinge (osteotomy cut depth)

The largest maximum principal (tensile) stresses occurred around the hinge axis in ROIs 1 and 2 (Figure 5-7). Contour maps of maximum principal strain demonstrated a similar pattern (Figures 6 and 7). Higher strain was experienced over a larger volume of bone when the intact hinge was largest (10mm) (Figures 6 and 7). A 10mm intact hinge produced the largest mean compressive (minimum principal) and tensile (maximum principal) strains (Table 2, Figure 8). However, the case with an intact hinge width of 10 mm is the only scenario where cortical bone strain did not exceed its yield strain ($8000\mu\epsilon$) across its transverse plane thickness (Figure 7). Decreasing the intact hinge to 5mm similarly concentrated maximum principal strain at the osteotomy apex but reduced the mean cortical bone maximum principal strain by 48% (Table 2). Minimum principal strain behaved similarly for cortical bone but for cancellous bone strain was highest for the 7.5mm hinge scenario. This may reflect different volumes of bone

occupying the ROI rather than a truly significant difference between 10mm and 7.5mm scenarios.

Maximum principal stresses (tensile) were higher in larger volumes of cortical bone for the larger 10mm intact hinge (Figures 5-7) with concentrations in both the lateral cortex and spreading vertically to the plateau (Figure 6). Reducing the intact hinge width concentrated maximum principal stress laterally and reduced stress experienced at the plateau (Figure 6). A similar pattern was seen for cancellous bone. As would be expected in an opening wedge osteotomy, minimum principal stresses (compressive) were largest at the external cortical bone surface at the level of the osteotomy (Figure 5) and were largest with the largest intact (10mm) hinge (Table 2). Using von Mises stress to reflect a scalar magnitude, ROI 1 showed larger stresses with larger intact hinges (Table 2). Greater cut depths with smaller remaining bone hinges required less force to obtain wedge opening of 10mm (Table 2 and 3, Figure 8a and b). However, deeper osteotomies leave a smaller volume of cortical bone to resist fracture (Figure 7).

Apical Drill holes

Adding an apical drill hole to the osteotomy centred on the hinge axis concentrated the cortical bone maximum principal strain to the region immediately surrounding the hole (Figures 5 and 6), reduced strain vertically to the plateau (Figure 6) and reduced transverse plane strain extending across the remaining cortical bone (Figure 7). The same was true for minimum principal strain. The net effect of this was a reduction in stresses and strains in ROI 1 for all drill holes, with greater reductions for greater diameter holes: mean Von Mises stress (2mm 11% reduction; 4mm 42%; 6mm 61%); mean minimum (2mm 8% reduction; 4mm 44%; 6mm

64%); and mean maximum principal strains (2mm 6% reduction; 4mm 35%; 6mm 55%) (Table 2). Cancellous bone stresses and strains were increased by blunting the apex with a 2mm drill hole, but decreased in holes of greater diameters (Table 3). The 6mm drill contacted and removed further cortical bone along the apex of the osteotomy leading to a cortical stress concentration which was not present in the smaller diameter drill holes (Figure 6). Though the drill holes effectively reduced the width of intact lateral bone, their effect in reducing bone strain in ROI 1 appeared to exceed that which would be expected by reducing hinge width alone (Figure 8b): the screw hole geometry appears to play an additional role. Despite a greater width of intact hinge compared to the 7.5mm (7.69mm) intact model, when a 4mm drill hole was employed with a subsequently larger intact hinge of 8.19mm, ROI strains were much reduced. Similarly, the 6mm drill hole removed only an additional 0.5mm of intact lateral hinge compared to the 7.5mm intact hinge model with no drill hole, but was associated with less than half the ROI 1 cortical bone strain.

Discussion

As the depth of osteotomy cut is increased and the remaining hinge of intact bone decreased, cortical bone stresses and strains become more concentrated at the osteotomy apex and horizontally focused with a reduced reaction force required for wedge opening. Shallower osteotomies leaving larger hinges of intact cortical bone result in greater strains extending to the joint surface, and presumably therefore a greater risk of fracture propagating vertically to the articular surface. Blunting the apex of the osteotomy with a drill hole decreases the associated local cortical bone strain in tension and compression. Increasing drill hole diameter further reduces local cortical and cancellous bone strains, stresses and the force required to

distract the osteotomy. This reduction in bone strain and reaction force is greater than would be expected for the associated reduction in intact hinge width alone that is associated with creating these holes. It is preferable for less force to be required to open the wedge to improve control, however, fracture may result if the intact bone hinge thickness is too small. There is similarly a balance between creating a more favourable strain environment to reduce the risk of unwanted fracture and preserving cortical bone stock to reduce fracture risk. It appears that, of the scenarios modelled, leaving an intact hinge of 10mm with a drill hole diameter of 4mm best achieves this balance and provides a 67% reduction in the force require to distract the osteotomy compared to when no axis drill hole is made.

As would be expected in an opening wedge osteotomy, maximum principal (tensile) stress and strain were concentrated at the apex hinge and the internal surface of the cortical bone with minimum principal (compressive) stress and strain concentrated on the external cortical bone surface. Higher stresses in the cortical than the cancellous bone are also expected: cortical bone has a higher Young's modulus and consequently carries more load on wedge opening. Though cancellous bone responses are included in this study, the prevention of unwanted cortical bone fracture is of greatest interest and thus cortical bone was the focus. As cortical bone is weaker in tension than compression and thus fracture primarily caused by tension, maximum principal stresses and strains have been used as our primary outcome measures.

Apical drill holes dissipated the articular surface strain concentrations and reduced the distraction force required. This suggests that apical drill holes would therefore reduce fracture risk, especially vertically to the joint surface. Managing crack tip stresses by blunting the osteotomy apex is expected to reduce the risk of accidental crack propagation and fracture.

When fracture occurs, construct stability is affected and time to union can be prolonged [10]. The osteotomy fixation plate experiences greater stresses and strains in the presence of fracture increasing the possibility of fatigue failure especially in delayed union [11].

The effect of an apical drill hole in opening wedge HTO has been investigated previously in an experimental biomechanical model, though Bujnowski et al[19] concluded no benefit in terms of cortical strain reduction or risk of lateral fracture in a cadaveric study of 14 paired specimens. Only one diameter of drill hole was investigated and cortical strain was measured at a single location using a single strain gauge. The advantage of the FE method is the potential to model multiple scenarios and explore strains in regions not limited to the external surface.

FE has previously been used to investigate various elements of HTO: plate type and construct stability[11, 20-23] and to optimise mechanical axis positioning[24]. Where FE models have previously been used to investigate apical drill holes, only stresses have been examined and results have been conflicting. Kaze et al.[25] identified reduced lateral cortex stresses with the addition of a 5mm diameter apical drill hole. In contrast, Carranza et al.[26] concluded that an apical drill hole increased stresses and fracture risk. Notably, both studies used von Mises stress as the primary outcome measure for comparison. It has been argued that yielding and damage in bone is best described using strain rather than stress, as strain based criteria are numerically more efficient and accurate than stress based criteria[27]. In exploring both directional stresses and strains, the current study identifies a useful role for apical drill holes in optimising the biomechanical environment at opening wedge HTO.

In the scenarios modelled here, an apical drill hole of ≥4mm diameter centred 10mm medial to the lateral cortex reduced both cortical and cancellous bone strains. Increasing the drill

diameter to 6mm removed excessive cortical bone along the length of the drill hole and should probably be avoided to maintain an adequate hinge. Similarly, the transverse plane contour maps highlight the amount of cortical bone removed to achieve a 5mm intact hinge. This should be borne in mind when judging osteotomy depth intraoperatively using 2D radiographs. Whilst achieving a narrow intact hinge reduces the associated stresses and strains, it markedly reduces both the margin of error and the force required to achieve this distraction (by 84% here) thus increasing the risk of fracture. In contrast, when larger distraction forces are required to achieve the desired wedge opening, surgical accuracy may be sacrificed with the risk of fracture if excessive force is applied.

Though many surgeons continue to perform osteotomies free-hand, computer assisted navigation [28-30] and patient specific jigs [31] are available to aid precision and accuracy. The option of an apical drill hole has been incorporated into some proprietary osteotomy jigs and this is supported by our results. In combination with patient specific plates [11] a drill hole technique could be used to maximally manipulate the strain environment of the proximal tibia during opening wedge osteotomy and fixation. From the biomechanical evidence available it appears that a drill hole of 2-3mm is insufficient to significantly alter the stress/strain environment of the proximal tibia at HTO, but that a drill hole of 4-5mm significantly affects this environment and may therefore reduce the risk fracturing, particularly laterally.

Limitations of this study include the use of a composite tibia. These do not reflect the graduated trabecular structure of proximal tibial cancellous bone, but are applicable to the "average" tibia [32]. Anisotropic, heterogeneous bone was modelled using isotropic and homogenous material

properties and a linearly elastic analysis was performed. This is a common method and does not discredit the differences found between osteotomy geometries [14]. Though bone is viscoelastic with non-linear behaviour [32,33], linear modelling can be used to reduce computing requirements when loading is not cyclical [27,35]. It is important to highlight that as this model assumes linear elasticity it is not possible to simulate fracture. Similar approaches using linear elasticity have previously shown to work well [36]. The use of strain based criteria rather than stress based criteria accommodates for material anisotropy and bone volume ratio (or porosity) – while yield stresses for bone are both anisotropy and porosity dependent, yield strains are largely uniform [27,37]. The partitioning of the ROIs may have affected the interpretation of results and conclusions may be different if different ROIs were used.

Conclusion

In conclusion, the addition of an apical drill hole to an opening wedge HTO reduces both compressive and tensile strains in the region surrounding the osteotomy apex and hinge axis and reduces the transmission of large strains vertically towards the articular surface. Based on the results of this composite tibia it appears that using a 4mm drill hole centred at a distance of 10mm from the intact lateral cortex maintains sufficient cortical bone and minimises local horizontal and more distant vertical strain and theoretically the risk of fracture. Incorporating such an apical drill hole reduces the force required to open the osteotomy thus making the distraction process more controlled. Pre-drilling the osteotomy apex is a simple technique which could be incorporated by surgeons performing both freehand or jig based HTOs.

References

[1] Arthritis Research UK. 2013. Osteoarthritis in General Practice. Available from: https://healthinnovationnetwork.com/wp-content/uploads/2017/01/Osteoarthritis_in_general_practice__July_2013__Arthritis_Research_UK_PDF_421_MB.pdf

[2] Arthritis Foundation. 2018. Arthritis by the numbers. Available from: https://www.arthritis.org/Documents/Sections/About-Arthritis/arthritis-facts-stats-figures.pdf

[3] Government of Canada. 2017. Most common types of arthritis. Available from: https://www.canada.ca/en/public-health/services/chronic-diseases/arthritis/most-common-types-arthritis.html

[4] Duffell L, Gulati, V, Southgate D, McGregor A. 2013. Measuring body weight distribution during sit-to-stand in patients with early knee osteoarthritis. Gait & Posture 38: 745–750.

[5] Mündermann A, Dyrby C, D'Lima D, et al. 2008. In vivo knee loading characteristics during activities of daily living as measured by an instrumented total knee replacement. Journal of Orthopaedic Research 26: 1167–1172.

[6] Scott C, Oliver W, MacDonald D, et al. 20. 2016. Predicting dissatisfaction following total knee arthroplasty in patients under 55 years of age. Bone and Joint Journal 98-B:1625-1634.

[7] Takeuchi R, Ishikawa H, Kumagai K, et al. 2012. Fractures around the lateral cortical hinge after a medial opening-wedge high tibial osteotomy: a new classification of lateral hinge fracture. *Arthroscopy* 28:85–94.

[8] Lee S, Nha K, Lee D. 2019. Posterior cortical breakage leads to posterior tibial slope change in lateral hinge fracture following opening wedge high tibial osteotomy. Knee Surgery, Sports Traumatology, Arthroscopy 27: 698-706.

[9] Ogawa H, Matsumoto K, Akiyama H. 2017. The prevention of a lateral hinge fracture as a complication of a medial opening wedge high tibial osteotomy. The Bone & Joint Journal 99: 887–893.

[10] Kumagai K, Yamada S, Nejima S, et al. 2019. Lateral hinge fracture delays healing of the osteotomy gap in opening wedge high tibial osteotomy with beta-tricalcium phosphate block. Knee [Epub ahead of print] doi: 10.1016/j.knee.2019.10.027.

[11] MacLeod AR, Serrancoli G, Fregly BJ, et al. 2018. The effect of plate design, bridging span, and fracture healing on the performance of high tibial osteotomy plates - an experimental and finite element study. Bone & Joint Research 7: 639–649.

12 Dessyn E, Sharma A, Donnez M, et al. 2019. Adding a protective k-wire during opening high tibial osteotomy increases lateral hinge resistance to fracture. Knee Surgery, Sports Traumatology, Arthroscopy. DOI: 10.1007. Available from: https://link-springer-com.ezproxy.is.ed.ac.uk/content/pdf/10.1007%2Fs00167-019-05404-7.pdf

[13] Csernatony Z, Kiss L, Mano S. 2008. A new technique of wedge osteotomy to diminish undesirable fractures. European Journal of Orthopaedic Surgery & Traumatology 18: 485–488.

[14] Scott CEH, Eaton MJ, Nutton RW, Wade FA, Evans SL, Pankaj P. Metal backed *versus* all polyethylene unicompartmental knee arthroplasty: the effect of implant thickness on proximal tibial strain in an experimentally validated finite element model. *Bone Joint Res* 2017: 6(1); 22-30

[15] Danese I, Pankaj P, Scott CEH. The effect of malalignment on proximal tibial strain in fixed bearing UKA: A comparison between metal backed *and* all-polyethylene components using a validated finite element model. *Bone Joint Res* 2019: 2;8(2):55-64.

[16] Bedford A, Liechti KM. 2000. Mechanics of Materials. Prentice Hall; p 528-531.

[17] Wolfram U, Schwiedrzik J. 2016. Post-yield and failure properties of cortical bone. BoneKEy Reports. DOI: 10.1038. Available from: https://www.ncbi.nlm.nih.gov/pmc/articles/PMC4996317/pdf/bonekey201660.pdf

[18] Kopperdahl DL, Keaveny TM. 1998. Yield strain behavior of trabecular bone. Journal of Biomechanics 31:. 601–608.

[19] Bujnowski K, Getgood A, Leitch K, et al. 2018. A pilot hole does not reduce the strains or risk of fracture to the lateral cortex during and following a medial opening wedge high tibial osteotomy in cadaveric specimens. Bone & Joint Research 7: 166–172.

[20] Koh YG, Son J, Kim HJ, et al. 2018. Multi-objective design optimization of high tibial osteotomy for improvement of biomechanical effect by using finite element analysis. Journal of Orthopaedic Research 36: 2956-2965.

[21] Izaham RMAR, Kadir MRA, Rashid AHA, et al. 2012. Finite element analysis of puddu and tomofix plate fixation for open wedge high tibial osteotomy. Injury 43: 898–902.

[22] Pauchard Y, Ivanov TG, McErlain DD, et al. 2015. Assessing the local mechanical environment in medial opening wedge high tibial osteotomy using finite element analysis. Journal of Biomechanical Engineering 137: 031005-1 – 031005-7.

[23] Koh YG, Son J, Kwon SK, et al. 2018. Biomechanical evaluation of opening-wedge high tibial osteotomy with composite materials using finite-element analysis. The Knee 25: 977–987.

[24] Martay JL, Palmer AJ, Bangerter NK, et al. 2018. A preliminary modeling investigation into the safe correction zone for high tibial osteotomy. The Knee 25: 286–295.

[25] Kaze AD, Maas S, Hoffmann A, Pape D. 2017. Mechanical strength assessment of a drilled hole in the contralateral cortex at the end of the open wedge for high tibial osteotomy. Journal of Experimental Orthopaedics 4: 1-19.

[26] Carranza VA, Reeves J, Getgood A, Burkhart TA. 2019. Development and validation of a finite element model to simulate the opening of a medial opening wedge high tibial osteotomy. Computer Methods in Biomechanics and Biomedical Engineering 22: 442-449.

[27] Pankaj P, Donaldson FE. Algorithms for a strain-based plasticity criterion for bone. *Int J Numer Methods Biomed Eng* 2013;29:40-61.

[28] Song SJ, Bae DK. 2016. Computer-assisted navigation in high tibial osteotomy. Clinics in Orthopedic Surgery 8: 349–357.

[29] Gebhard F, Krettek C, Hüfner T, et al. 2011. Reliability of computer-assisted surgery as an intraoperative ruler in navigated high tibial osteotomy. Archives of orthopaedic and trauma surgery 131: 297–302.

[30] Reising K, Strohm PC, Hauschild O, et al. 2013. Computer-assisted navigation for the intraoperative assessment of lower limb alignment in high tibial osteotomy can avoid outliers compared with the conventional technique. Knee Surgery, Sports Traumatology, Arthroscopy 21: 181–188.

[31] TOKA 2019. OA in the 21st century. Available from: https://www.toka.org.uk/discover-toka/for-surgeons/

[32] Cristofolini L, Viceconti M. Mechanical validation of whole bone composite tibia models. *J Biomech* 2000;33:279-288.

[33] Manda K, Xie S, Wallace RJ, Levrero-Florencio F, Pankaj P. Linear viscoelasticity - bone volume fraction relationships of bovine trabecular bone. *Biomech Model Mechanobiol* 2016;15:1631-1640.

[34.] Manda K, Wallace RJ, Xie S, Levrero-Florencio F, Pankaj P. Nonlinear viscoelastic characterization of bovine trabecular bone. *Biomech Model Mechanobiol* 2017;16:173-189.

[35] Conlisk N, Howie CR, Pankaj P. 2015. The role of complex clinical scenarios in the failure of modular components following revision total knee arthroplasty: A finite element study. Journal of Orthopaedic Research 33: 1134-1141.

[36] Goffin JM, Pankaj P, Simpson AH. 2014. Are plasticity models required to predict relative risk of lag screw cut-out in finite element models of trochanteric fracture fixation?. Journal of Biomechanics 47: 323-328.

[37] Levrero-Florencio F, Margetts L, Sales E, et al. Evaluating the macroscopic yield behaviour of trabecular bone using a nonlinear homogenisation approach. *J Mech Behav Biomed Mater* 2016;61:384-396.

Table 1. The number of cortical and cancellous bone elements for each model

Number of elements	Intact bone hinge			Drill hole		
	10mm	7.5mm	5mm	2mm	4mm	6mm
Cortical	101,976	96,169	88,778	102,215	107,089	111,201
Cancellous	140,453	104,419	99,530	140,796	140,529	141,992

Table 2. Comparison of mean stress and strain criteria in ROI 1 for different osteotomy depths.

ROI 1	Unit	Intact bone hinge		
		10mm	7.5mm	5mm
Mean Von Mises stress				
Cortical	MPa	243.3	216.5	111.1
Cancellous	MPa	4.5	3.7	0.6
Mean Maximum Principal Strain				
Cortical	%	1.0	1.00	0.52
Cancellous	%	3.3	2.4	0.3
Mean Minimum Principal Strain				
Cortical	%	-1.0	-0.9	-0.5
Cancellous	%	-0.9	-1.0	-0.2
Reaction Force for wedge opening	kN	0.70	0.35	0.6

Table 3. Comparison of mean stress and strain criteria in ROI 1 for different drill holes.

Mean in ROI 1	Unit	No drill hole	Drill hole		
			2mm	4mm	6mm
Von Mises stress					
Cortical	MPa	243.3	216.1	141.3	95.4
Cancellous	MPa	4.5	6.5	3.4	3.3
Maximum Principal Strain					
Cortical	%	1.0	0.94	0.65	0.45
Cancellous	%	3.3	4.60	2.33	2.25
Minimum Principal Strain					
Cortical	%	-1.0	-0.92	-0.56	-0.36
Cancellous	%	-0.9	-1.42	-0.79	-0.64
Reaction Force for wedge opening	kN	0.70	0.50	0.23	0.11

Figure Legends

Figure 1. The osteotomy geometry in coronal and sagittal planes for the 10mm intact hinge scenario. White dotted lines represent the anatomical axis of the tibia and an additional line perpendicular to this in the coronal plane at the level of the fibular head (fibular not included). The osteotomy was thus 15° from this line in the coronal plane, and parallel to the native tibial slope in the sagittal plane (yellow dotted lines).

Figure 2. The transverse plane of the proximal tibia as cut along the white dotted line indicated in the coronal plane image in figure 1. The red dotted line represents the anatomical tibial rotation, and the white dotted line parallel to this the apex of the osteotomy created. The distance d was varied to model intact hinges of width 5-10mm. Drill holes were similarly made along this white dotted line.

Figure 3. The creation of apical drill holes. The midpoint of the osteotomy apex for the 10mm intact lateral hinge model was identified (yellow circle) and drill holes of 2, 4 and 6mm diameter were centred on this axis along the line indicated in Figure 2 to create 3 new models including drill holes.
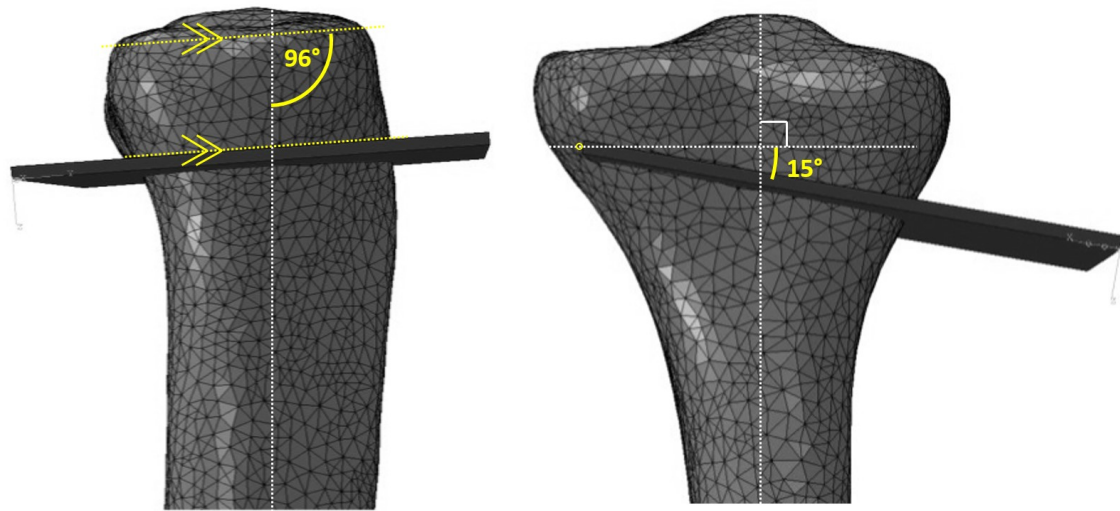
Figure 4. The proximal tibia was partitioned along 2 planes creating 4 regions of interest (ROIs): 2mm superiorly offset from the osteotomy; and 2mm medially offset from the osteotomy apex. A biased mesh was generated by ROI.

Figure 5. Contour plots of the cortical bone surface seen from the posterior aspect with maximum principal (positive indicates tension) and minimum principal (negative indicates compression) stress (GPa) for each cut depth and drill hole diameter.
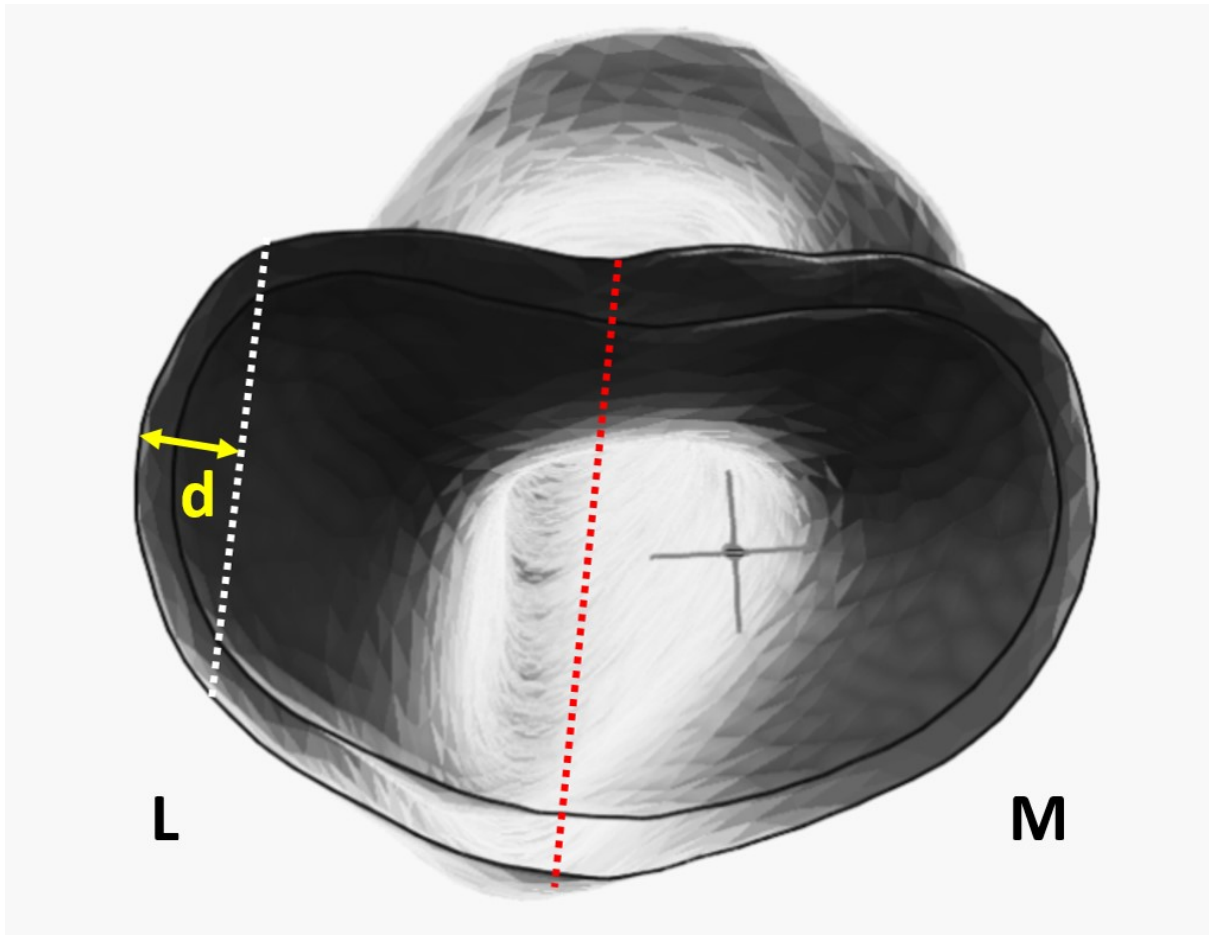
Figure 6. Contour plots of regions of interest 1 and 2 seen in the mid-coronal plane with maximum principal stress (GPa) and strain for each cut depth and drill hole diameter.

Figure 7. Contour plots of the intact hinge (located in ROI 1) in the transverse plane with maximum principal (tension) stress (GPa) and strain for each cut depth and drill hole diameter.

Figure 8. Mean maximum and minimum principal strains in region of interest 1 for each intact hinge width and drill hole scenario with the corresponding reaction force required to obtain 10mm of osteotomy opening a) x axis ordered by scenario, b) x axis ordered by remining hinge width intact.
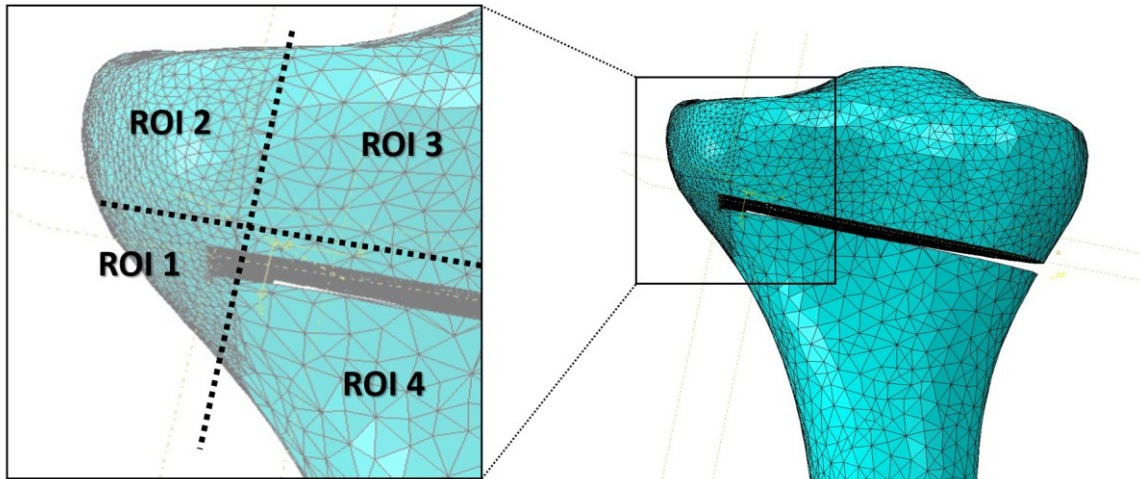
Figure 1. The osteotomy geometry in coronal and sagittal planes for the 10mm intact hinge scenario. White dotted lines represent the anatomical axis of the tibia and an additional line perpendicular to this in the coronal plane at the level of the fibular head (fibular not included). The osteotomy was thus 15° from this line in the coronal plane, and parallel to the native tibial slope in the sagittal plane (yellow dotted lines).
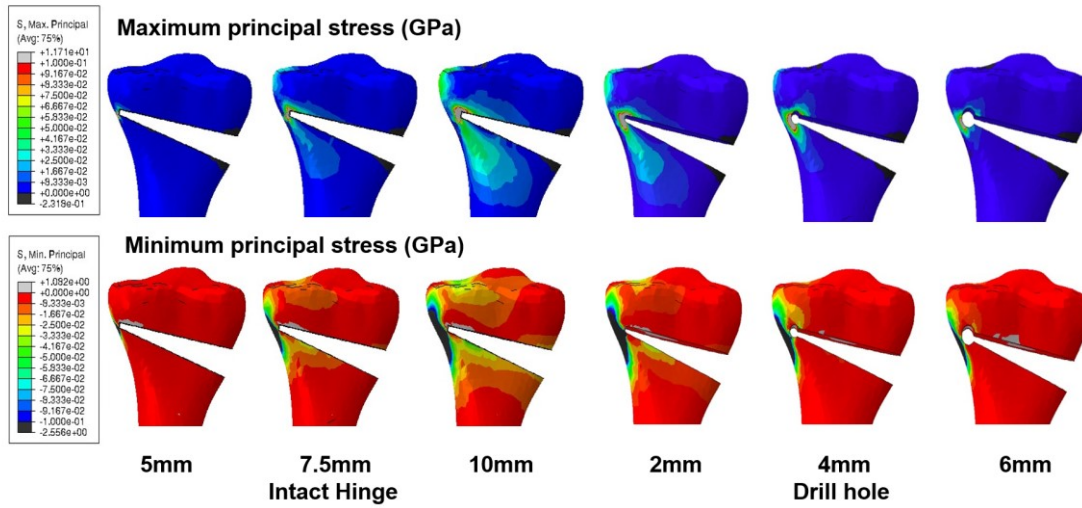
Figure 2. The transverse plane of the proximal tibia as cut along the white dotted line indicated in the coronal plane image in figure 1. The red dotted line represents the anatomical tibial rotation, and the white dotted line parallel to this the apex of the osteotomy created. The distance d was varied to model intact hinges of width 5-10mm. Drill holes were similarly made along this white dotted line.
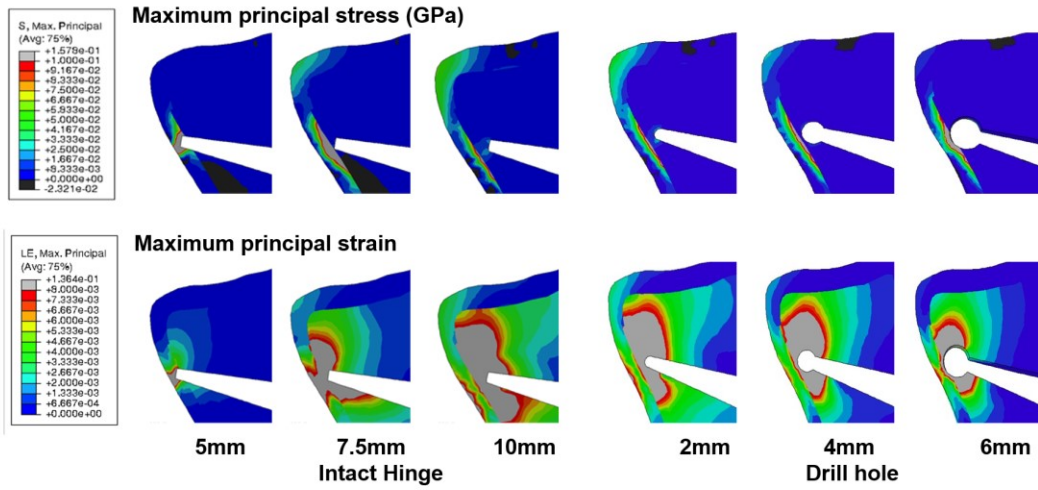
Figure 3. The creation of apical drill holes. The midpoint of the osteotomy apex for the

10mm intact lateral hinge model was identified (yellow circle) and drill holes of 2, 4 and

6mm diameter were centred on this axis along the line indicated in Figure 2 to create 3 new

models including drill holes.

Figure 4. The proximal tibia was partitioned along 2 planes creating 4 regions of interest (ROIs): 2mm superiorly offset from the osteotomy; and 2mm medially offset from the osteotomy apex. A biased mesh was generated by ROI.
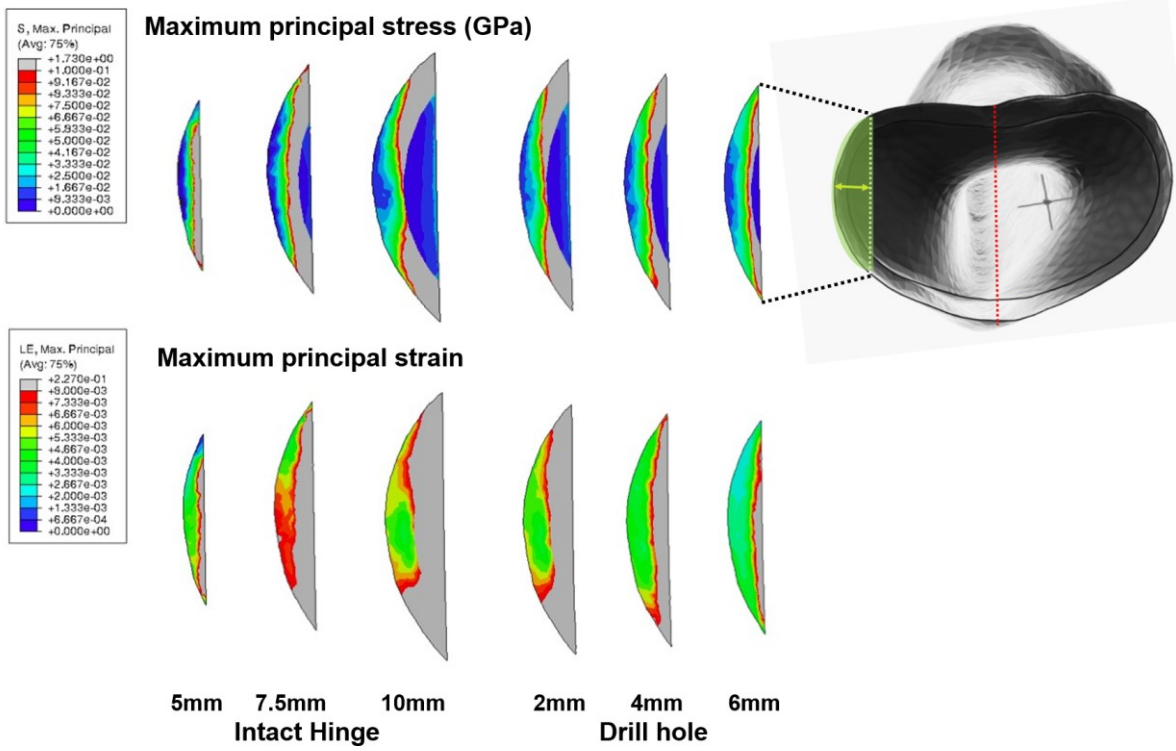
Figure 5. Contour plots of the cortical bone surface seen from the posterior aspect with maximum principal (positive indicates tension) and minimum principal (negative indicates compression) stress (GPa) for each cut depth and drill hole diameter.
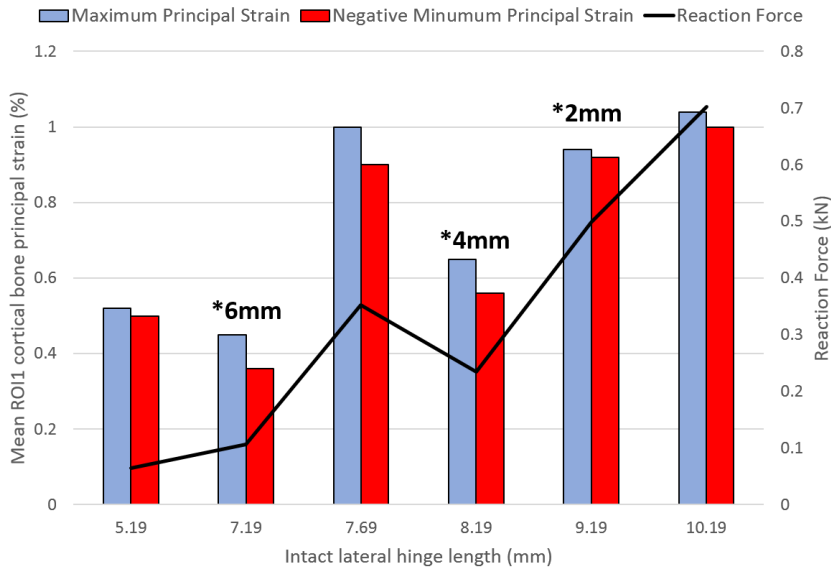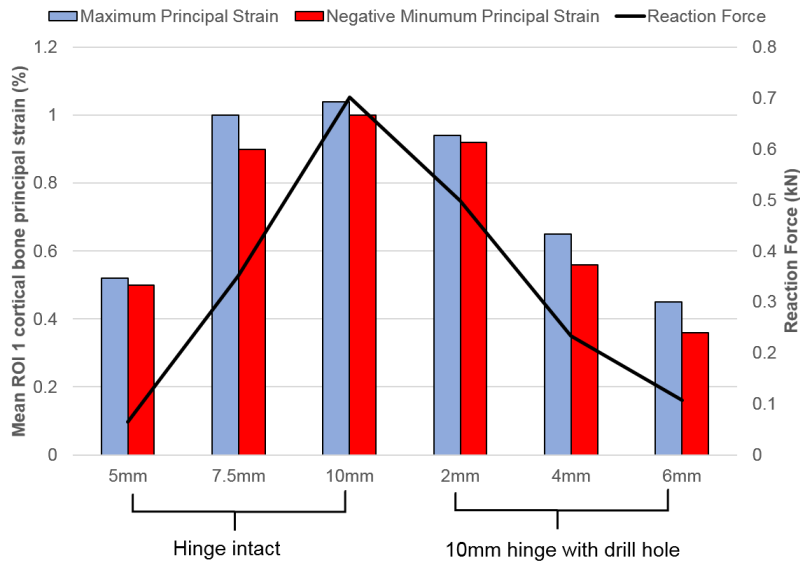
Figure 6. Contour plots of regions of interest 1 and 2 seen in the mid-coronal plane with maximum principal stress (GPa) and strain for each cut depth and drill hole diameter.

Figure 7. Contour plots of the intact hinge (located in ROI 1) in the transverse plane with maximum principal (tension) stress (GPa) and strain for each cut depth and drill hole diameter.

Figure 8. Mean maximum and minimum principal strains in region of interest 1 for each intact hinge width and drill hole scenario with the corresponding reaction force required to obtain 10mm of osteotomy opening a) x axis ordered by scenario, b) x axis ordered by remining hinge width intact.